

DO NOT COPY
submitted to
EGWR 2000
DO NOT DISTRIBUTE

A Geometrical Approach to Modeling Reflectance Functions of Diffracting Surfaces

Nicolas Tsingos

Bell Laboratories

tsingos@research.bell-labs.com

Abstract. Modeling light reflection off surfaces, although extensively studied in computer graphics, remains a challenging problem when simulating wave phenomena. In particular, diffraction has received little attention until very recently, when an analytical model based on the wave theory of light was proposed [24].

It is commonly believed in the computer graphics community that diffraction phenomena cannot be captured using a ray-based theory of light. However, an extension to geometrical optics, known as the *Geometrical Theory of Diffraction* (GTD), was introduced in 1962, giving a solution to the problem.

In this paper, we give an introduction to the GTD and show that this theory can be successfully used to derive procedural shaders for simple diffracting surfaces. We also discuss how the GTD can be integrated into a ray-based virtual gonio-spectro-photometer to derive Bidirectional Reflectance Distribution Functions incorporating diffraction effects for more general types of surfaces.

1 Introduction

Simulation of surface reflectance properties continues to be one of the important and challenging aspects of photo-realistic computer graphics. Two types of approaches have been proposed to model surface properties: analytical methods and distributed ray-tracing estimations (virtual gonio-spectro-photometry).

Analytical methods derive analytical formulas for the surface Bidirectional Reflectance Distribution Function (BRDF), usually using the Kirchhoff integral theorem and statistical properties of the surface micro-geometry (typically modeled as a random height-field) [7]. Although most analytical approaches are limited to isotropic surfaces, several extensions have been proposed for anisotropic surfaces, as in [9]. Poulin and Fournier [17] simulate small cylinders added to (or subtracted from) the surface to model anisotropy. Finally, Ward [26] fits analytical models to measurements for a given class of materials: reflected light is in this case measured from a real sample using a gonio-spectro-photometer. Until recently, no wave effects (*e.g.* interference, diffraction) were modeled. In 1992, Smits and Meyer described an analytical model treating thin film interference [22]. In 1999, Stam [24] introduced a unified analytical model, based on the scalar Kirchhoff integral theorem, dealing with anisotropy and diffraction caused by micro-gratings on the surface. He can treat more general, non-random height fields by relating the scattered intensity to the spectral density of a function of the surface height. The major advantage of analytical approaches is that they are computationally efficient and usually offer some control parameters. Their main drawback is the lack of generality since they model surfaces as height fields. While remaining a valid assumption in most cases, this limitation prevents modeling of more complex, layered or pigment-based, materials.

Distributed ray-tracing approaches are inspired by measurement methods which use a real gonio-spectro-photometer. They basically simulate such a physical setup by casting a large number of incident rays on a sample 3D model of the surface micro-geometry [2, 27, 6]. The rays are traced as they are reflected or refracted inside the micro-model. Their contributions are accumulated in a direction-dependent structure when they exit the sample. The operation is repeated for each possible incident direction thus leading to the sampled BRDF of the material. The major advantage of such techniques is that they impose no restriction on the surface micro-geometry, allowing to model complex layered surfaces. However, they are very time consuming, solve the problem for one particular surface and, similar to real measurements, lead to a very large data set. Thus, further processing is usually needed to either fit an analytical model to these virtual measurements or to compress the information using directional basis functions (spherical harmonics, wavelets, *etc.*) [2, 27, 20]. Distributed ray-tracing is usually applied on the *milliscale* geometry (feature size around 0.1 mm) for which classic ray optics is a valid approximation. This means that the local behavior of the surface must already be approximated by some reflectance function that models the *microscale* effects (feature size around 1 μm) [27]. Consequently, interference and diffraction are rarely considered explicitly, since they should be taken into account on the microscale level. Several approaches have been proposed to model interference due to layered media or pigments in a ray-tracing context [4, 5, 19]. They deal with microscale features, such as pigments in iridescent paints, which scattering effects cannot be modeled by previous analytical models. In this context, only Snell's law is used for local reflection/refraction but rays carry phase information and possibly polarization information [28, 25] used to obtain interference. However, none of the previous work incorporating wave phenomena considered diffraction which is likely to have a strong influence at this scale. This is mainly due to the lack of a model describing the effects of diffraction in a geometrical ray formalism.



Fig. 1. A picture computed with our GTD diffraction shader. The surface micro-geometry is a grating and colors are the result of interference between several diffracted paths.

In this paper we show that diffraction effects can be modeled with a geometrical ray-based approach. Indeed, in 1962, Joseph Keller introduced an extension of geometrical optics to account for diffraction phenomena: the Geometrical Theory of Diffraction (GTD) [11]. Curiously, this theory seems to have received little attention in optics and does not appear in classic optics monographs [8, 1], while it has been extensively used and refined in radio-wave channel modeling and acoustics [10, 14, 18, 12].

In the first section we present an overview of the Geometrical Theory of Diffraction (GTD). In particular, we show how new geometrical paths are introduced to account for

diffraction effects and how to compute their contribution. We then present an application of this theory to modeling reflection off diffracting surfaces. In section 3 we use the GTD to build procedural “diffraction shaders” for particular types of micro-geometry acting as diffraction gratings (*e.g.* a compact disc). In section 4, we discuss how the GTD can be incorporated in a more complex distributed ray-tracing framework, allowing the treatment of diffraction effects in virtual gonio-spectro-photometers. Finally, we discuss some limitations and further refinements of the proposed approach.

2 Computing the wedge-diffracted light field using the GTD

The Geometrical Theory of Diffraction (GTD) [11] adds diffraction effects to the ray theory of light. It assumes that wedges (*i.e.* an edge and a pair of adjacent polygons) act as secondary sources, scattering new diffracted rays. The diffracted field is obtained by summing the contribution of these new rays, taking their relative phase into account. Colorful diffraction patterns are created by the interferences between all possible propagation paths (*i.e.* combinations of reflections and diffraction). Similar to reflected rays, diffracted rays follow Fermat's principle: if the propagation medium is homogeneous, the rays follow the shortest path from the source to the receiver, stabbing the diffracting edges. For a point source, a point receiver and any sequence of combined diffractions by edges and specular reflections off surfaces, this defines a unique path. Besides, for every wedge, incident and diffracted rays make equal angles with the edge direction¹. Equivalently, a ray incident on a diffracting edge gives rise to a cone of diffracted rays all around the edge (Figure 2), the existence of which has been verified experimentally [21]. Diffracted rays follow the laws of geometrical optics and can therefore be reflected and diffracted before reaching the receiver. They are subject to binary visibility tests and their contribution is removed if they hit an obstacle.

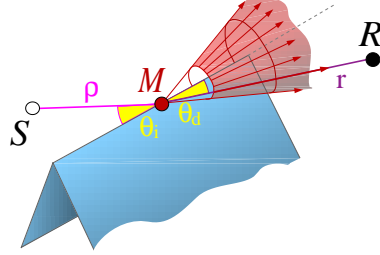


Fig. 2. Rays diffracted by a 3D wedge. At oblique incidence, an incoming ray gives rise to a cone of diffracted rays whose central axis is the edge. The aperture angle of the cone θ_d is equal to the angle between the incident ray and the edge θ_i . At normal incidence ($\theta_i = \frac{\pi}{2}$), diffracted rays form a disk of omnidirectional coplanar rays in a plane orthogonal to the edge.

Each diffracted ray is modulated by a diffraction coefficient in the same way a reflected ray is modulated by a reflection coefficient. The GTD alone does not give an expression for the diffraction coefficient. Keller obtained a result in the case of a wedge, by identification of his solution with an exact analytical solution previously obtained by Sommerfeld [23]. Unfortunately, Keller's coefficient becomes singular as the diffracted direction grazes geometrical shadow regions or specular reflection boundaries created

¹ If the incident ray gets diffracted into a different medium, the usual law of refraction applies to the incident and diffracted angles.

by the wedge (Figure 3). In 1974, Kouyoumjian and Pathak gave a new, well defined expression for the diffraction coefficient in their Uniform Geometrical Theory of Diffraction (UTD) [13, 16]. We used this expression in our implementation (see Appendix A for the exact expression). It can be observed that the diffraction coefficient amplitude increases with the wavelength. Thus, low frequencies get more diffracted than high frequencies, which is coherent with the fact that for high frequencies (relative to the feature size) classic geometrical optics remains a good approximation.

The contribution of a diffracted ray to the total field at the receiving point for plane wave incidence is given by:

$$\begin{aligned}\mathcal{E}_{\text{diffracted}}(R) &= \mathcal{E}_{\text{incident}}(M) \hat{D} e^{ikr}, \\ &= A \hat{D} e^{ik(\rho+r)}\end{aligned}\quad (1)$$

where R is the receiver location, M is the diffraction point on the edge, $k = 2\pi/\lambda$ is the wave number, λ is the wavelength, A is the amplitude of the incident wave, and \hat{D} is the diffraction coefficient, calculated according to the UTD. The complex exponential accounts for the classic phase variation along the ray, which depends on the total optical path length $\rho + r$ (see also Figure 3 for other notations). The diffraction coefficient, \hat{D} , is itself a complex number accounting for amplitude and phase changes due to diffraction and depends on both the incident and diffracted direction on the edge and the corresponding angles θ_i , α_i and α_d (Figures 2, 3 and Appendix A). These parameters can be determined using an edge fixed coordinate system and one of the two wedge surfaces as reference, as shown on Figure 3.

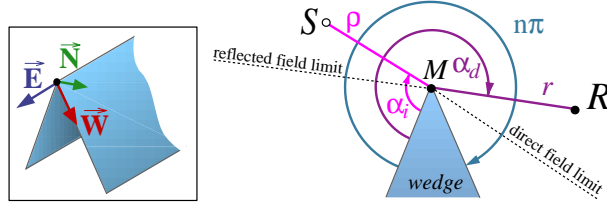


Fig. 3. Notations and edge-fixed coordinate system definition for the Uniform GTD wedge diffraction coefficient. The choice of the wedge surface used as reference is arbitrary and will not change the value of the diffraction coefficient.

Unfortunately, finding the diffraction paths is similar to a well known NP-complete motion planning problem [3]: finding a 3D shortest path avoiding polyhedral obstacles. We are not interested here in finding the absolute shortest path but rather a shortest path going through an edge for every diffraction event (or possibly a sequence of edges and surfaces for multiple combinations of reflections and diffractions). However, this problem has no simple solution in the general case. In the next section we show that it can be solved explicitly for a number of specific situations and present some results.

3 Building diffraction shaders using the GTD

GTD can be used to create procedural diffraction shaders by constructing explicitly the diffraction paths for all diffracting wedges present in the microgeometry. In our experiments, we limited ourselves to direct diffraction (*i.e.* we do not treat diffraction of reflected rays or further reflection of diffracted rays).

The problem is to evaluate the diffracted component of the field, according to Eq. (1), for given ingoing and outgoing directions. Our solution is to build, for every

```

Spectrum computeDiffractedField( Vector in, Vector out )

Spectrum Result; Vector diffPoint;
Vector SRC = FAR_DIST*(-in);
Vector DEST = FAR_DIST*out;
complex S[NB_WAVELENGTHS];
For every wavelength  $\lambda$     S[ $\lambda$ ] = 0.0;
For every wedge WEDGE
| float length = findShortestPath(WEDGE,SRC,DEST,&diffPoint);
| For every wavelength  $\lambda$ 
| | complex D = diffractionCoefficient(SRC,DEST,diffPoint,WEDGE, $\lambda$ );
| | float k =  $2*\pi/\lambda$ ;
| | S[w] += D * ei*k*length;
For every wavelength  $\lambda$     Result[ $\lambda$ ] = |S[ $\lambda$ ]|2;
return Result;

```

Fig. 4. Pseudo-code for a GTD shader. The procedure **findShortestPath** finds the shortest path (if not obstructed) between the two points SRC and DEST that stabs the edge of the wedge W. It returns the length of the path and the diffraction point on the edge. The parameter FAR_DIST is a distance that should be chosen large compared to the feature size of the micro-geometry. The procedure **diffractionCoefficient** computes the diffraction coefficient as given in Appendix A.

possible wedge in the micro-geometry, the shortest path, stabbing the edge and connecting a point source and a point receiver (assumed to be “far away” from the surface, w.r.t. the wavelength) along the ingoing and outgoing directions. Figure 5 (c) illustrates this process. Its two major difficulties are finding the path and determining its visibility to the receiver. In the case of single wedge diffraction, an explicit geometrical construction exists for the diffracted path [11]. We first rotate the source and receiving point around the edge so that both points and the edge lie in the same plane. Then the intersection between the source/receiver line and the edge gives the diffraction point. From this construction, we obtain both the path length and a diffraction point on the edge. An approximation to the shortest path can also be obtained through a distance minimization process such as a binary search along the edge. Once the path is found, we check that it does not intersect any obstacles. Finally, we compute the diffraction coefficient according to the location of the diffraction point and use the path length to compute interference between all contributions. The pseudo-code in Figure 4 summarizes the whole procedure.

Figure 6 shows results of applying this approach to a CD-like surface. The micro-geometry is modeled as continuous parallel strips (Figure 5 (a) and (b)). A procedural GTD shader, based on the algorithm in Figure 4, is called for every pixel corresponding to a diffracting surface. We set parameter FAR_DIST to $10000 \mu\text{m}$. Paths are generated for 2000 “tracks” (i.e. 4000 wedges) which correspond roughly to an extent of 3mm (Figure 5 (c)).

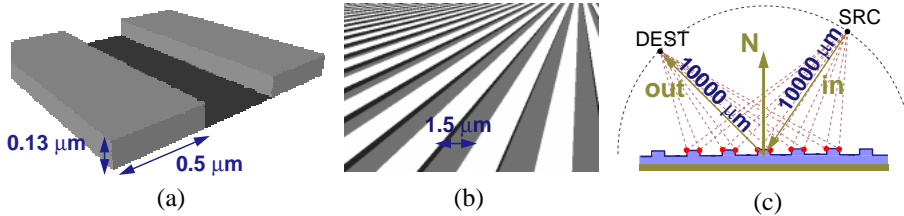


Fig. 5. Micro-geometry and diffracted paths used for our CD-like diffraction shader. (a) and (b): We model the micro geometry of a CD-like surface by parallel strips. (c) For the 2 silhouette edges of each strip we build a shortest path, passing through the edge, which connects a point source and point receiver “far away” from the surface in the incoming and outgoing direction.

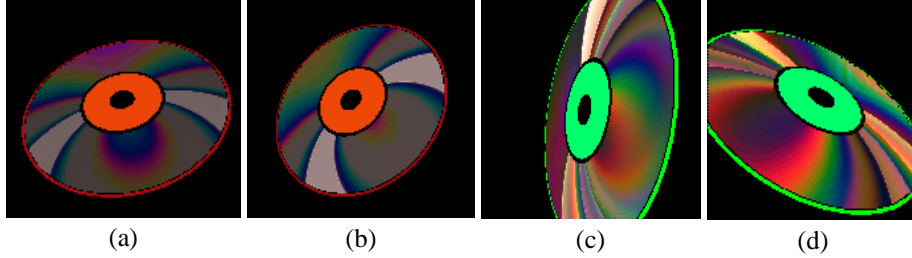


Fig. 6. Example of diffraction patterns from directional light sources. Pictures (a) and (b) use a directional lighting normal to the CD surface and were computed with 20 wavelengths. Pictures (c) and (d) use 3 directional sources and were computed using 40 wavelengths.

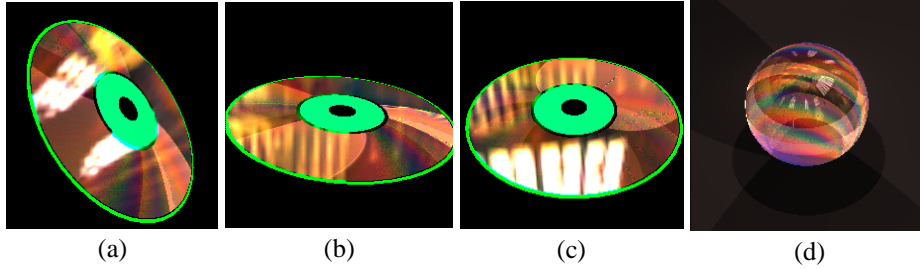


Fig. 7. Examples with an additional environment map (40 wavelengths). (a) and (b) use 3 directional sources for the direct lighting. (c) and (d) use 3 point sources. Note: the environment map is not used as a global radiance map.

We deal with the anisotropic orientation of the tracks across the surface by associating with every point a local referential [9, 24]. This referential is used to rotate the in and out directions when evaluating the shader. In Figure 7, we added a mirror specular component to the shader and used it to access an environment map. The images are 200×200 pixels (no oversampling) and computed using 40 wavelengths. We used a uniform subdivision of the visible light spectrum between 380 and 775 nm. The resulting color effects are due to the interferences between all diffraction paths at each wavelength (all sources have flat spectra). We tested two approaches for finding the shortest path. First, using the explicit geometrical technique, computing times for the pictures in Figure 7 range from 3 to 5 hours. Using a binary search for each of the 4000 diffracting edges, computing times range between 7 and 16 hours (SGI R10000 195MHz) for similar picture quality. In the later case, we used an accuracy of $10^{-6} \mu\text{m}$ to check the convergence of the iterative minimization process. It is likely that a greater threshold could be used but we did not investigate this point further, since we wanted to make sure the interference effects are properly taken into account.

4 Extension to a distributed ray-tracing framework and discussion

In the previous section, we built the diffraction paths explicitly, knowing that such paths are of minimal length amongst all possible paths stabbing the wedges. The advantage of an explicit construction is that it is aliasing free. However, it is very time consuming and is not applicable to complex surfaces or higher orders of combined reflection and diffraction. Another approach, more suited to such applications, would be to construct the paths implicitly, exploiting the fact that a ray impinging on a wedge will give rise

to a cone of diffracted rays. Thus, a distributed ray-tracing approach, similar to the previous work on virtual gonio-photometry, could be easily extended to take into account diffraction effects. When a ray hits an edge, random diffracted rays are generated that lie on the diffraction cone and their contributions are modulated by the corresponding diffraction coefficients. To limit aliasing problems due to the computation of edge/ray intersections, “thick” rays have to be used. Such an approach has been used with success for radio wave channel modeling in urban environments [18, 12].

The GTD is in essence an approximation to the exact solution of the wave equation and is limited to cases where the size of the geometrical features is larger than the wavelength. It is not straightforward to derive quantitative validity conditions and thus to predict if the model is going to give satisfying results (at least from a perceptual realism point of view). The theory proved to be useful for radio waves and acoustics. From the experiments we ran, we are optimistic that the GTD can give good results for computer graphics applications. However, an implementation in a ray-casting based framework would lead to a more accurate model, since multiple scattering could be easily taken into account (in the case of a highly reflective material such as a CD metallic coating layer, multiple scattering is likely to have a strong influence).

In this paper, we restricted ourselves to scalar wave theory and assumed surfaces were perfectly reflecting. Extensions to the original GTD theory can be found in [13, 15, 16] to account for vector waves (*i.e.* polarization) and absorbent surfaces. The major drawback of the GTD is that the expression of the diffraction coefficient is only known for wedges. However, no limitation is placed on the micro-geometry and thus any polygonal model could be used. For more complex geometries and especially curved surfaces, the theory becomes highly complicated since rays comprising segments of geodesic curves on the surfaces must be constructed.

5 Conclusion

Contrary to popular belief, geometrical techniques exist to handle diffraction phenomena. In this paper, we showed that the Geometrical Theory of Diffraction can be successfully used in computer graphics to create diffraction shaders. We focused on experimenting with simple situations to verify the applicability of the theory, which is in essence an approximation to the exact solution of the wave equation. From those experiments, we are convinced that this theory could be used in computer graphics applications to model BRDFs of complex diffracting surfaces. Since the GTD is based on the geometrical optics principles, it can be used to complement existing ray-casting based virtual gonio-spectro-photometry approaches. Consequently, it will allow for treating more general surfaces and help derive new improved analytical models.

Acknowledgments

The author would like to thank Steve Fortune for enlightening discussions on shortest path problems and geometrical issues related to the GTD. Many thanks also to Gopal Pingali for his valuable suggestions and Agata Opalach for her help with the figures and for proofreading the paper.

A Computing diffraction coefficients

The Uniform GTD [13, 16] expresses the scalar wave diffraction coefficient for an infinite wedge and hard boundary conditions on perfectly reflecting surfaces as:

$$\begin{aligned} \hat{D}(n, k, r, \theta_i, \alpha_i, \alpha_d) = & -\frac{e^{-i\frac{\pi}{4}}}{2n\sqrt{2k\pi}\sin\theta_i} \\ & \left[\tan^{-1}\left(\frac{\pi+(\alpha_d-\alpha_i)}{2n}\right) F(kLa^+(\alpha_d-\alpha_i)) \right. \\ & + \tan^{-1}\left(\frac{\pi-(\alpha_d-\alpha_i)}{2n}\right) F(kLa^-(\alpha_d-\alpha_i)) \\ & + \left\{ \tan^{-1}\left(\frac{\pi+(\alpha_d+\alpha_i)}{2n}\right) F(kLa^+(\alpha_d+\alpha_i)) \right. \\ & \left. \left. + \tan^{-1}\left(\frac{\pi-(\alpha_d+\alpha_i)}{2n}\right) F(kLa^-(\alpha_d+\alpha_i)) \right\} \right], \end{aligned} \quad (2)$$

where (see also Figures 2 and 3)

- k is the wave number. $k = 2\pi/\lambda$,
- n is such that the exterior wedge angle is $n\pi$,
- ρ is the source to diffraction point distance,
- r is the receiver to diffraction point distance,
- θ_i is the angle between
the edge vector \overrightarrow{E} and the incident direction. $\theta_i \in [0, \pi]$,
- α_i is the angle between vector \overrightarrow{W}
and the incident direction. $\alpha_i \in [0, n\pi]$,
- α_d is the angle between vector \overrightarrow{W}
and the diffracted direction. $\alpha_d \in [0, n\pi]$,

and where:

$$F(X) = 2i\sqrt{X}e^{iX} \int_{\sqrt{X}}^{+\infty} e^{-i\tau^2} d\tau, \quad (3)$$

$$L = r \sin^2 \theta_i \text{ for plane wave incidence,} \quad (4)$$

$$a^\pm(\beta) = 2 \cos^2 \left(\frac{2\pi n N^\pm - \beta}{2} \right), \quad (5)$$

N^\pm is the integer that satisfies more closely the relations:

$$2\pi n N^+ - \beta = \pi \quad \text{and} \quad 2\pi n N^- - \beta = -\pi \quad (6)$$

We refer the reader to [10, 13, 16] for useful details regarding how to implement the computation of this coefficient, in particular to evaluate the Fresnel integral in Eq.(3).

References

- [1] M. Born and E. Wolf. *Principles of Optics*. 7th edition, Pergamon Press, 1999.
- [2] B. Cabral, N. Max, and N. Springmeyer. Bidirectional reflection functions from surface bump maps. *ACM Computer Graphics, Annual conference series, SIGGRAPH'87 Proceedings*, p. 273-281, 1987.
- [3] J. Canny and J. Reif. New lower bound techniques for robot motion planning problems. *Proc. 28th IEEE Symposium on Foundations of Computer Science*, p. 49-60, 1987.
- [4] M. L. Dias. Ray tracing interference color. *IEEE Computer Graphics and Applications*, 11(2):54-60, 1991.
- [5] J. S. Gondek, G. W. Meyer, and J. G. Newman. Wavelength dependent reflectance functions. *ACM Computer Graphics, Proc. SIGGRAPH'94*, p. 213-220, 1994.

- [6] P. Hanrahan and W. Krueger. Reflection from layered surfaces due to subsurface scattering. *ACM Computer Graphics, SIGGRAPH '93 Proceedings*, p. 165-174, 1993.
- [7] X. D. He, K. E. Torrance, F. X. Sillion, and D. P. Greenberg. A comprehensive physical model for light reflection. *Computer Graphics (SIGGRAPH 91)*, 25(4):175-186, 1991.
- [8] E. Hecht. *Optics*. 3rd edition, Addison Wesley, 1998.
- [9] J. Kajiya. Anisotropic reflection models. *ACM Computer Graphics, Annual conference series, SIGGRAPH'85 Proceedings*, p. 15-21, 1985.
- [10] T. Kawai. Sound diffraction by a many sided barrier or pillar. *J. of Sound and Vibration*, 79(2):229-242, 1981.
- [11] J. Keller. Geometrical theory of diffraction. *J. of the Optical Society of America*, 52(2):116-130, 1962.
- [12] S. Kim, B. Guarino, T. Willis, V. Erceg, S. Fortune, R. Valenzuela, L. Thomas, J. Ling, and J. Moore. Radio propagation measurements and prediction using three-dimensional ray tracing in urban environments at 908 MHz and 1.9 GHz. *IEEE Trans. on Vehicular Technology*, 48:931-946, 1999.
- [13] R. G. Kouyoumjian and P. H. Pathak. A uniform geometrical theory of diffraction for an edge in a perfectly conducting surface. *Proc. of IEEE*, 62:1448-1461, 1974.
- [14] U. Kurze. Noise reduction by barriers. *J. of the Acoustical Society of America*, 55(3):504-518, 1974.
- [15] D. I. Laurenson. *Indoor Radio Channel Propagation Modelling by Ray Tracing Techniques*. PhD thesis, University of Edinburgh, 1994.
- [16] D. McNamara, C. Pistorius, and J. Malherbe. *Introduction to the Uniform Geometrical Theory of Diffraction*. Artech House, 1990.
- [17] P. Poulin and A. Fournier. A model for anisotropic reflection. *ACM Computer Graphics, Annual conference series, SIGGRAPH'90 Proceedings*, p. 273-282, 1990.
- [18] A. Rajkumar, B. Naylor, F. Feisullin, and L. Rogers. Predicting RF coverage in large environments using ray-beam tracing and partitioning tree represented geometry. *Wireless Networks*, 2(2):143-154, 1996.
- [19] M. Schramm, J. Gondek, and G. Meyer. Light scattering simulations using complex sub-surface models. *proceedings of Graphics Interface'97, Kelowna (B.C.), Canada*, 1997.
- [20] P. Schröder and W. Sweldens. Spherical wavelets: Efficiently representing functions on the sphere. *ACM Computer Graphics, Annual conference series, SIGGRAPH'95 Proceedings*, p. 161-172, 1995.
- [21] T. Senior and P. Uslenghi. Experimental detection of the edge diffraction cone. *Proc. of the IEEE (Letters)*, 60(11):1448, 1972.
- [22] B. E. Smits and G. Meyer. Newton's colors: Simulating interference phenomena in realistic image synthesis. In K. Bouatouch and C. Bouville, Ed., *Photorealism in Computer Graphics (Proceedings Eurographics Workshop on Photosimulation, Realism and Physics in Computer Graphics, 1990)*, p. 185-94, 1992.
- [23] A. Sommerfeld. *Optics*. Academic Press, Inc., New York, 1954.
- [24] J. Stam. Diffraction shaders. *ACM Computer Graphics, Proc. SIGGRAPH'99*, p. 101-110, 1999.
- [25] D. Tannenbaum, P. Tannenbaum, and M. Wozny. Polarization and birefringency considerations in rendering. *ACM Computer Graphics, SIGGRAPH '94 Proceedings*, p. 221-222, 1994.
- [26] G. Ward. Measuring and modeling anisotropic reflection. *ACM Computer Graphics, Annual conference series, SIGGRAPH'92 Proceedings*, p. 265-272, 1992.
- [27] S. H. Westin, J. R. Arvo, and K. E. Torrance. Predicting reflectance functions from complex surfaces. *Computer Graphics (SIGGRAPH 92)*, 26(2):255-264, 1992.
- [28] L. B. Wolff and D. J. Kurlander. Ray tracing with polarization parameters. *IEEE Computer Graphics and Applications*, 10(6):44-55, 1990.